NANO LETTERS

2007
Vol. 7, No. 1
143−148

Two Distinct Buckling Modes in Carbon Nanotube Bending

Xiaojie Duan,[†] Chun Tang,[‡] Jin Zhang,*[,†] Wanlin Guo,*[,‡] and Zhongfan Liu*[,†]

Beijing National Laboratory for Molecular Sciences, Key Laboratory for the Physics and Chemistry of Nanodevices, Centre for Nanoscale Science and Technology, College of Chemistry and Molecular Engineering, Peking University, Beijing 100871, China, and Institute of Nano Science, Nanjing University of Aeronautics and Astronautics, Nanjing 210016, China

Received October 15, 2006

ABSTRACT

By using controlled SPM manipulation, carbon nanotubes have been continuously bent into a series of increasing angles, and two distinct buckling modes corresponding to "abrupt" and "gradual" buckle formation were observed through recording the height increment at the bend site during the loading process. Molecular dynamics simulation also found the two buckling modes in different types of carbon nanotubes, and their atomistic mechanism was revealed. Finally, the dependence of the critical buckling condition on diameters of carbon nanotubes was tentatively studied.

The buckling behavior is a fundamental mechanical property of carbon nanotubes (CNTs). It is found that the electrical conductance and the effective bending modulus of CNTs will be significantly changed by the formation of a buckle.[1,2] This makes a comprehensive understanding of the buckling occurrence such as the buckling mode and critical buckling condition important for future applications of CNTs in the nanoelectromechanical system (NEMS) and superstrong composite materials.[3,4] Compared to the abundant theoretical efforts concerning the buckling behavior of CNTs,[2,5−7] the direct experimental study is limited due to the small dimension of CNTs. Although the existence of the buckle in bent single- and double-walled carbon nanotubes[6] and the wavelike wrinkle in multiwalled carbon nanotubes (MWNTs)[8] has been determined by high-resolution transmission electron microscopy (HRTEM) and scanning probe microscopy (SPM),[9,10] the experimental report on the buckle formation process and critical buckling condition and their dependence on tube structures is still limited. The limitation mainly lies in the difficulty in controlled deforming of the carbon nanotubes.

In the present study, the structure evolution of individual carbon nanotubes in the bending process is systematically investigated through continuously bending the tubes to different angles by SPM manipulation. Measurements of the height change at the buckling site show two distinct buckling modes: the abrupt transition from uniform elastic bending to buckling at a critical bending angle accompanying a height jump and the gradual transition with the height increasing slowly. Using molecular dynamics (MD) simulations, the two buckling modes are consistently reproduced in different types of CNTs, and the atomistic mechanism of the two modes is revealed. Furthermore, a special "dual-size" effect concerning the important role of tubes thickness and diameter in determining their buckling modes was predicted. Finally, the dependence of the critical buckling condition on diameters of carbon nanotube was tentatively studied.

All carbon nanotubes used in our bending experiments were grown directly on silicon (111) surfaces with a 200 nm thick SiO_2 layer by chemical vapor deposition (CVD). Briefly, $Fe(OH)_3$ colloids hydrolyzed from $FeCl_3$ were spin-coated onto silicon surfaces to act as the catalysts, and the carbon nanotube growth was carried out at 775 °C for 5 min with a flow of ethene at 10 standard cubic centimeters per minute (sccm) and hydrogen and argon at 600 sccm, respectively. The carbon nanotubes prepared using this direct surface growth are free from defects and contamination of amorphous carbon.[11,12] The diameter of the as-grown carbon nanotubes is mainly in the range of 1−2 nm with a few exceptions. For the bending test, straight ends of carbon nanotubes with different diameters were purposely chosen. All carbon nanotubes here can be manipulated repeatedly without any cleavage. This proves that they are individual carbon nanotubes rather than bundles.

The SPM bending manipulation was conducted using a Nanoscope III SPM (Veeco) with specifically compiled software (see Supporting Information). Normally, the SPM

* Corresponding authors. E-mail: jinzhang@pku.edu.cn (J.Z.); zfliu@pku.edu.cn (Z.L.); wlguo@nuaa.edu.cn (W.G.).
[†] Peking University.
[‡] Nanjing University of Aeronautics and Astronautics.

10.1021/nl062424i CCC: $37.00
Published on Web 12/07/2006

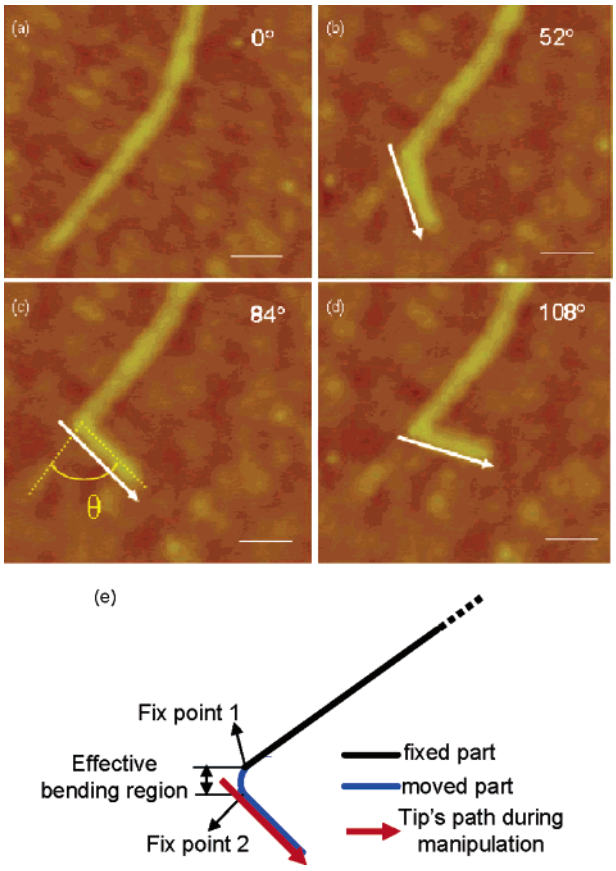

Figure 1. Tapping-mode AFM height images of a carbon nanotube bent to different angles. The angles between the initial and final position of the moved part was defined as the bending angle θ as shown in panel c. In the top right corner of each image, the bending angles are shown. During the manipulation, the end segment has been pushed along the path shown by the white arrows. The direction and position of the tube end segment was determined by the tip's path, which made it possible to control the bending angle. Scale bar: 50 nm. (e) Schematic figure of the detailed bending structure of carbon nanotubes. There is only vdW interaction between the substrate and the moved part indicated by the blue line.

was operated in tapping atomic force microscopy mode in air. For a typical bending manipulation, the tip was pressed down about 5−20 nm with the feedback switched off for an optimal contact load at the tip−sample interface. After that, the tip moved horizontally along a predefined straight path, which had a small angle with the axis of the end segment that would be manipulated (as shown by the white arrow in Figure 1) and pushed the end segment that had a typical length of about 100 nm. Then the tip returned to the normal imaging distance, and the feedback was switched on to get the images of the bent tubes.[13,14] All the height measurement from the AFM image was conducted with a linear fit of the substrate profile as captured, without plane fitting.[15] The diameter values were an average of more than 10 points along the tubes. Figure 1 shows typical bending results of a carbon nanotube with a diameter of 1.31 nm. It can be seen that the position and direction of the manipulated segment was definitely determined by the tip's path. In our system, because of the straight manipulation path, the main part of the moved segment was straight and the effective bending segment was localized in a small region, which appeared as the cross point of the fixed and moved part due to the AFM resolution limitation.[16] We define the angle between the manipulated part and its initial position as the bending angle θ, which is closely related with the curvature of the effective bending region. By simply predefining the tip path during manipulation, the bending angle could be controlled, which made the observation of the structure evolution in the whole bending process possible. The bending configuration was maintained by the interaction between tubes and substrate.

Table a in Figure 2 shows the heights of the bend "point" at different bending angles of this tube. An increment in height was caused by the first manipulation to 26°. Actually, this elevation happened for the entire moved segment. This can be seen from the section analysis in Figure 2c: in the black profile, there was no difference in the height of the bend "point" and the straight moved part, while in the red profile, the height of the bend "point" was obviously larger than that of the fixed part. The elevation of the moved part caused by the first manipulation in fact occurred in all carbon nanotubes we manipulated. In the following manipulation, the straight manipulated part would remain at this elevated height all the time. For the bend "point", as long as the bending had not reached the critical buckling condition, this elevated height would also remain constant. This height increment may be caused by the interaction decrease between the substrate and the manipulated CNTs segment compared to that between the substrate and the as-grown CNTs, as proved by the smaller force (less pressing-down distance of tip) needed to achieve the following manipulation than the first manipulation. Because of the smaller interaction of substrate with the moved part than with the fixed part, the bending strain would propagate along the moved segment rather than the fixed segment, and the effective bending region would locate in the moved segment, which interacted with the substrate only by van der Waals (vdW) force. It has been proved that this vdW interaction had no significant influence on CNT buckling behavior, as discussed in the following text. The schematic figure of the detailed bending structure can be found in Figure 1e.

To take this elevation into account when studying CNT buckling behavior, for the ΔH (increment in height) values, except for the bending angle 0° where it had been set as 0, other values at the bend "point" for all CNTs in this paper were calculated by a comparison with the values after the first manipulation (an average of the bend "point" heights at all bending angles before buckling) rather than the initial heights. The plot of the ΔH vs the bending angles for the tube with a diameter of 1.31 nm is shown in panel (b) of Figure 2. After the first manipulation, the height remained nearly constant until reaching 96°. As opposed to the case at bending angle 26°, the height increase at 96° only happened at the bend "point" when an obvious protuberance appeared. This can also be seen from the 3-D AFM height images (Figure S1a, Supporting Information). The height jump suggested a transition from uniform elastic bending to buckling of CNTs happened at a certain bending stage between 84° and 96°. This is consistent with the theoretical

a

Bending angle (Degree)	H (nm)	ΔH (nm)
0	1.31	0
26	1.66	0.02
43	1.56	-0.08
52	1.66	0.02
58	1.66	0.02
66	1.65	0.01
77	1.65	0.01
84	1.65	0.01
96	1.94	0.30
108	1.90	0.26

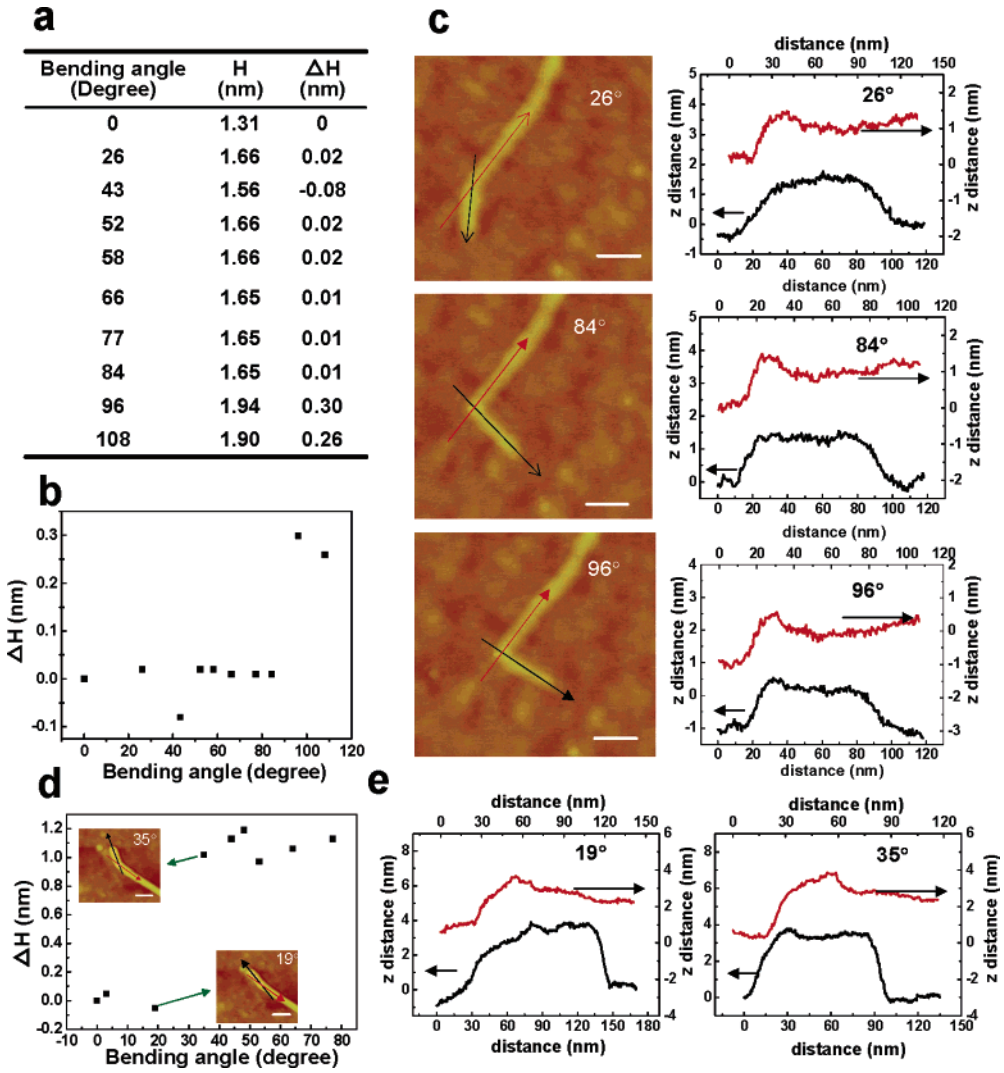

Figure 2. (a) Heights and height changes (ΔH) at the bend "point" of carbon nanotube with diameter of 1.31 nm at different bending angles. (b) Plot of ΔH vs bending angles. The red and black lines in the right panels of (c) correspond to the profiles marked with the red and black arrows in the left panels, respectively. In table a, because there was no height change before manipulation, the ΔH has been set as zero at 0°. All the following ΔH was obtained from a comparison with the average value of heights from 26° to 84° before buckling. (d) Plot of ΔH at the bend "point" of carbon nanotube with diameter of 3.17 nm vs bending angles. The insets are the AFM images of this tube at 19° and 35°. (e) Section analysis of tube with diameter of 3.17 nm at 19° and 35°. The red and black lines correspond to the profiles marked with the red and black arrows in the inset of d, respectively. All the scale bars in the AFM height images are 50 nm.

predictions: when the bending strain is small, the C−C bonds of CNTs have a slight stretch at the outer side of the bending region and a compression at the inner side, which appears as uniform elastic bending. This structure has no significant difference with straight tubes. When the strain is increased to a certain extent, a new pattern, buckling, would be formed accompanying a minimization of the strain energy.[5,6] This structure has a special atomic arrangement as compared to the normal carbon nanotubes. For this tube, this transition was abrupt and it caused a height increment of 0.28 nm (an average of the ΔH for all bending angles after buckling, same for the following tubes). In subsequent bending to 108°, the buckle structure was preserved with the height constant again. The result here observed the transition from uniform elastic bending to buckling of an individual carbon nanotube experimentally, and the critical buckling angle appeared to be in the range of 84−96° for this tube.

Another case is shown for a carbon nanotube with a diameter of 3.17 nm (Figures 2d,e and S1b, Supporting Information). When bent to 35°, the newly formed protuberance at the bend "point" indicated the occurrence of buckling. The critical buckling angle for this tube was therefore in the range of 19−35°, and the final ΔH corresponding to the buckle formation was 1.08 nm. We have designated this abrupt transition from uniform bending to a fully formed buckle, as exhibited by the above two tubes, "buckling mode I".

As opposed to the abrupt transition from uniform elastic bending to a fully formed buckle, some carbon nanotubes had another buckling behavior. Figure 3a,b shows the bending results for a carbon nanotube with a diameter of 2.82 nm. The difference lay in that, from 50° to 91°, the height had experienced a gradual increase before reaching the final constant value rather than an abrupt jump. From

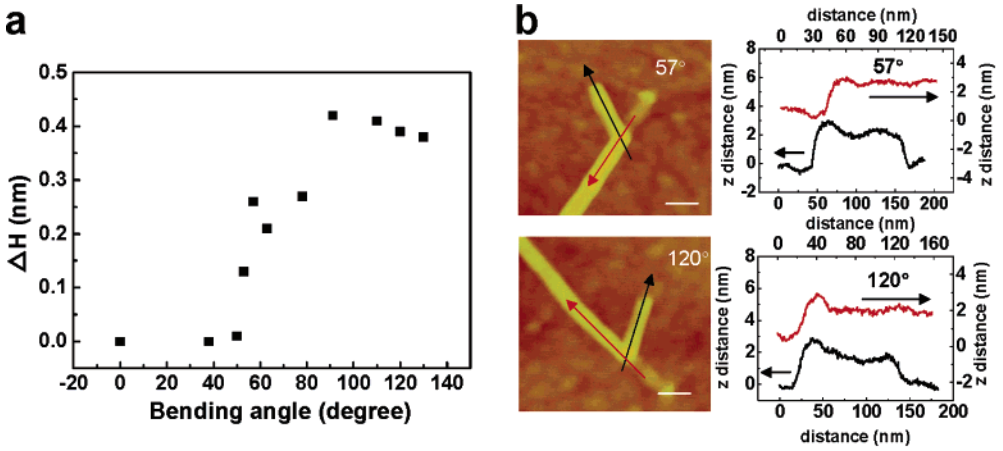

c

	mode I				mode II	
diameter (nm)	0.99	1.24	1.31	3.17	2.82	4.52
ΔH_{max} (nm)	0.20	0.32	0.28	1.08	0.40	1.00
critical angle (degree)	96-107	60-78	84-96	19-35	50-53, 78-91	<=16, 92-102

Figure 3. (a) Plot of ΔH at the bend "point" of carbon nanotube with diameter of 2.82 nm vs bending angles. It can be seen that there is a gradual increase in height from 50° to 91°. The red and black lines in the right panels of (b) correspond to the profiles marked with the red and black arrows in the left panels, respectively. From section analysis b and 3-D AFM height images (Figure S1c, Supporting Information), it can be seen that there is a small buckle formed at 57°, while at 120°, the buckle has been fully formed corresponding to the larger and stable protuberance at the bend site. All the scale bars in the AFM height images are 50 nm. Table c shows the critical buckling condition ranges and maximum height increment ΔH_{max} of different carbon nanotubes. For the two tubes of mode II, the first range is where the buckling begins and the second is where the buckling finishes.

the section analysis, it can be seen that, during this stage, for example at 57°, a small protuberance has been produced, while above 91°, the protuberance was larger and stable. The final maximum ΔH was 0.40 nm for this tube. This implied that the CNTs have experienced a series of intermediate states when transiting from the uniform elastic bending to the fully formed buckle. This was quite distinct from buckling mode I; we have designated this "buckling mode II".

By comparing the carbon nanotubes listed in table c of Figure 3, it was found that buckling mode I often happened for small-diameter CNTs, while mode II mainly occurred for larger-diameter tubes. To understand the atomistic mechanism of the two distinct buckling modes described above and also to explore their possible origin, molecular dynamics (MD) studies were conducted on CNTs of different types under bend loadings. In our MD simulations, the second-generation reactive empirical-bond-order potential was adopted. It was developed for hydrocarbons on the basis of the Tersoff−Brenner expression, and the L-J potential describing long-range vdW interaction was also included.[17,18] Three-walled, double-walled, and single-walled carbon nanotubes were modeled in this study. The bend loading was applied by giving a displacement of 0.2 Å to one end of the CNTs at each step, and then relaxing the whole system while keeping both ends of the CNTs fixed.

The two buckling modes were also observed by the simulations, and it was found that buckling mode I could be mainly observed in SWNTs, while buckling mode II mostly occurred in MWNTs, which have thicker tube walls than SWNTs. Panel a in Figure 4 presented the ΔH with respect to the bending angles of the (9,9) SWNT, which has a diameter of 1.21 nm and a length of 24.5 nm. Before 39°, a small ΔH increase happened and the configuration of the bent tube had no significant change except for a slight ovalization of the cross section. This means that the SWNT underwent uniform elastic bending during this stage. Typical geometrical configuration was shown as the lower inset. At 41°, a sudden jump from 0.199 to 0.448 nm happened in ΔH, which corresponded to the abrupt transition from uniform elastic bending to buckling, as shown by the geometrical configuration in the upper inset. This phenomenon was qualitatively consistent with the experimental buckling mode I, and simulations on other SWNTs such as the (8,8), (17,0), and (14,14) SWNTs led to the same conclusion.

As for MWNTs, several double-walled and three-walled carbon nanotubes were modeled in our studies. Unlike SWNTs, all MWNTs in our simulations showed a gradual buckling process. As exampled by the (4,4)/(9,9)/(14,14) MWNT shown in Figure 4b, a gradual height increase happened that corresponded to a series of buckling intermediate states formation. Typical geometrical configurations at 23° and 30° were shown in the inset. It could be found that there was nearly no buckling for the inner layers, and the outer layers were partly buckling compared to the full buckling of corresponding tubular graphene layers in SWNTs.

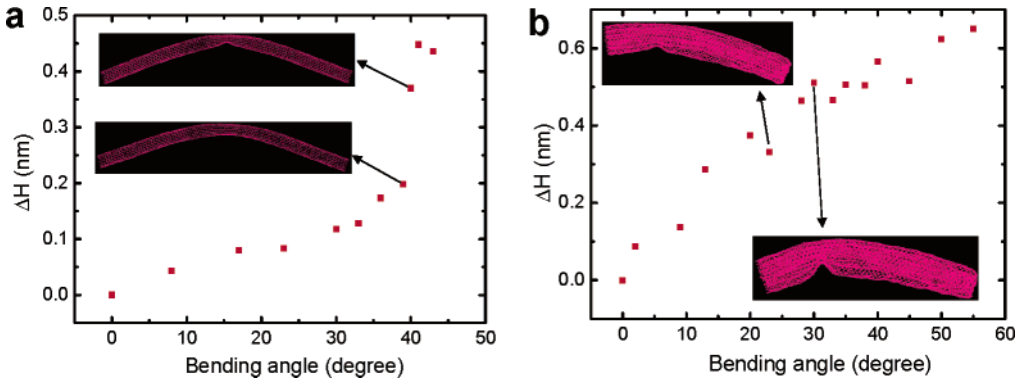

Figure 4. Molecular dynamics simulation results of carbon nanotubes under bend loadings. (a) Plot of ΔH vs bending angles of (9,9) SWNT, which is 1.21 nm in diameter and 24.5 nm in length. The sharp jump in ΔH can be observed from 39° to 41°. Insets are the representative geometrical configurations before (lower, 39°) and after (upper, 41°) buckling. (b) Plots of ΔH vs bending angles of (4,4)/(9,9)/(14,14) MWNT, which is 1.9 nm in diameter and 12.2 nm in length; ΔH increases gradually during the whole process. Typical configurations of the intermediate buckling states are shown as the insets, which are under 23° and 30° bending, respectively.

Along with the increase of the bending angles, the buckling of all individual layers proceeded gradually. This was in agreement with the experimental results of buckling mode II.

The inhomogeneity of the buckling state between the inner and outer layers in MWNTs indicated the important role of thickness in tube-buckling behavior. As predicted by the theoretical studies, the critical buckling curvature of CNTs is closely related to their diameters (for example, it was found that, for SWNTs, the critical buckling curvature is inversely proportional to the square of tube diameter[5]). Thicker CNTs would have larger difference in inner and outer wall diameters. Thus at some bending stages, the outer wall would buckle first, while the inner walls remained stable. Furthermore, the radial elastic modulus of carbon nanotubes also increased with decreasing diameter.[19] The less-deformed inner tube would offer strong restraint to prevent the outer tube from dramatic deforming in transverse directions. Different layers buckled at different bending stages, and the partial buckling of outer layers operated together and resulted in the gradual buckling of MWNTs. Here, it can be seen that, for carbon nanotubes such a nanoscale object, the vdW interaction began to show significant influence on their mechanical property and made their buckling behavior distinct from the macroscopic shells. Furthermore, both the experiment and simulation indicated that special CNT structures may be developed during the bending process. This diversity of structures may have potential applications in future NEMS or other nanoelectronic devices.[3]

The thickness should not be the only factor influencing the CNT buckling behavior. Considering small-diameter SWNTs, although the interwall vdW does not exist, the vdW interaction between the inner and outer side of the bending from the same wall could become remarkable and may offer a restriction for the buckling. While if the diameters of MWNTs were large enough and their walls were not too thick, the difference in critical buckling conditions for the inner and outer walls may be negligible, so all the walls may buckle simultaneously and the inner tube would offer less constraint to hinder the outer tube's deformation. Their buckling behavior may be more like mode I. The above analysis may explain the result of the tube that buckled as mode I while it had a diameter of 3.17 nm. So for the CNT buckling behavior, the thickness and diameter may have a cooperative effect. This cooperative effect has been proved by Chang et al. by using a molecular mechanics model.[7] The dependence of carbon nanotube properties on diameter could be regarded as a size effect, which is known as an important factor leading to special electronic, optical, magnetic, and chemical properties of nanomaterials.[20] Here, a special "dual-size" effect, diameter and thickness, which operated together to determine the CNT buckling behavior, may exist. This concept may be important for describing CNT mechanical properities.

In a slightly different case from the isolated CNTs in simulation, there was vdW interaction between the substrate and the effective bending region of tubes in the experiment. However, by using molecular dynamics simulation, it has been proved that this vdW interaction had no significant influence on tube buckling (Supporting Information). That is why such a good agreement between experimental and theoretical results had been achieved.

By comparing the range of the critical angles of the four carbon nanotubes buckling as mode I in table c of Figure 3, it is found that the critical angles decreased along with the increase of the carbon nanotube diameters except those with diameters of 1.24 and 1.31 nm. The trend here was consistent with the theoretical predictions,[5] where an inverse relation between the critical buckling curvature and the square of carbon nanotube diameters has been proposed, although the clear relationship between the critical angles and diameters could not be deduced by far here. The deviation of the carbon nanotubes with diameters of 1.24 and 1.31 nm may arise from the influence of the helicity, which has also been theoretically predicted for carbon nanotubes less than 2.0 nm in diameter.[6] Note that the critical angles in this study from experimental observations are much larger than those in the MD simulations and that reported by Iijima et al.[6] The reason for the difference may be due to the larger length of the experimental effective bending region corresponding to the manipulation process here, which resulted in larger bending angles for the same curvature. For the carbon nanotubes

buckling as mode II, there existed two characteristic bending angles: the angle where the buckle began to form and where the buckle had been fully formed. It is reasonable to speculate that the two angles were closely related to the structure details of the carbon nanotubes such as the diameter and thickness. The controlled bending of carbon nanotubes by SPM manipulation here may provide an effective way for investigating this dependence, and further work for illustrating this relation is still needed.

In summary, by using controlled SPM manipulation, carbon nanotubes have been continuously bent to a series of increasing angles and the transition from uniform elastic bending to buckling has been investigated. Two distinct modes corresponding to "abrupt" and "gradual" buckling were found. Using molecular dynamics (MD) simulation, the two buckling modes are consistently reproduced in different types of CNTs and their atomistic mechanism has been revealed. Furthermore, it was predicted that both the thickness and diameter of CNTs would contribute to their buckling modes, which resulted in a special "dual-size" effect in carbon nanotube buckling behavior. For the carbon nanotubes buckling as mode I, the critical angles decreased with increasing diameters. The work here investigated the whole bending process of CNTs and observed experimentally their transition from uniform elastic bending to buckling. The intermediate buckling states may have potential applications in future NEMS or other nanodevices, and the concept of the "dual-size" effect proposed here may be important for describing CNT mechanical properties. Furthermore, the strategy of using SPM manipulation to illustrate CNT deformation behavior may also be extended to other kinds of strain or other materials such as CNT-based composite materials, where the mechanical properties play an important role for their practical performance.[4,21,22]

Acknowledgment. This work was supported by NSFC (20573002), MOST (2006CB0N0701), The Fund for Creative Research Groups (50521201), NSFC, and FOKYING TUNG Education Foundation (94012). W. L. Guo acknowledges financial support from NSFC (10372044) and the Jiangsu Province NSF.

Supporting Information Available: Bending carbon nanotubes by SPM, supplementary data, molecular dynamics study of vdW interaction effect on CNTs buckling. This material is available free of charge via the Internet at http://pubs.acs.org.

References

(1) Postma, H. W. C.; Teepen, T.; Yao, Z.; Grifoni, M.; Dekker, C. *Science* **2001**, *293*, 76.
(2) Pantano, A.; Boyce, M. C.; Parks, D. M. *Phys. Rev. Lett.* **2003**, *91*, 145504.
(3) Cheng, H. M. *Carbon Nanotubes: Synthesis, Microstructure, Properties and Applications* ; Chemical Industry Press: Beijing, 2002.
(4) Munoz, E.; Dalton, A. B.; Collins, S.; Kozlov, M.; Razal, J.; Coleman, J. N.; Kim, B. G.; Ebron, V. H.; Selvidge, M.; Ferraris, J. P.; Baughman, R. H. *Adv. Eng. Mater.* **2004**, *6*, 801.
(5) Yakobson, B. I.; Brabec, C. J.; Bernholc, J. *Phys. Rev. Lett.* **1996**, *76*, 2511.
(6) Iijima, S.; Brabec, C.; Maiti, A.; Bernholc, J. *J. Chem. Phys.* **1996**, *104*, 2089.
(7) Chang, T. C.; Guo, W. L.; Guo, X. M. *Phys. Rev. B* **2005**, *72*, 064101.
(8) Poncharal, P.; Wang, Z. L.; Ugarte, D.; de Heer, W. A. *Science* **1999**, *283*, 1513.
(9) Falvo, M. R.; Clary, G. J.; Taylor, R. M.; Chi, V.; Brooks, F. P.; Washburn, S.; Superfine, R. *Nature* **1997**, *389*, 582.
(10) Wong, E. W.; Sheehan, P. E.; Lieber, C. M. *Science* **1997**, *277*, 1971.
(11) He, M. S.; Duan, X. J.; Wang, X.; Zhang, J.; Liu, Z. F.; Robinson, C. *J. Phys. Chem. B* **2004**, *108*, 12665.
(12) Wang, X.; Yue, W. B.; He, M. S.; Liu, M. H.; Zhang, J.; Liu, Z. F. *Chem. Mater.* **2004**, *16*, 799.
(13) Duan, X. J.; Zhang, J.; Ling, X.; Liu, Z. F. *J. Am. Chem. Soc.* **2005**, *127*, 8268.
(14) Ling, X.; Zhu, X.; Zhang, J.; Zhu, T.; Liu, M. H.; Tong, L. M.; Liu, Z. F. *J. Phys. Chem. B* **2005**, *109*, 2657.
(15) The measurement error was within 0.1 nm.
(16) Postma, H. W. C.; Sellmeijer, A.; Dekker, C. *Adv. Mater.* **2000**, *12*, 1299.
(17) Brenner, D. W. *Phys. Rev. B* **1990**, *42*, 9458.
(18) Brenner, D. W.; Shenderova, O. A.; Harrison, J. A.; Stuart, S. J.; Ni, B.; Sinnott, S. B. *J. Phys.: Condens. Matter* **2002**, *14*, 783.
(19) Li, C. Y.; Chou, T. W. *Phys. Rev. B* **2004**, *69*, 073401.
(20) Andrievski, R. A.; Glezer, A. M. *Scr. Mater.* **2001**, *44*, 1621.
(21) Laborde-Lahoz, P.; Maser, W.; Martinez, T.; Benito, A.; Seeger, T.; Cano, P.; de Villoria, R. G.; Miravete, A. *Mech. Adv. Mater. Struct.* **2005**, *12*, 13.
(22) Chen, W.; Tao, X. M.; Xue, P.; Cheng, X. Y. *Appl. Surf. Sci.* **2005**, *252*, 1404.

NL062424I